



Non-isothermal crystallization kinetics of graphite-reinforced crosslinked high-density polyethylene composites

Dimitra Kourtidou¹ · Evangelia Tarani¹ · Ioulia Chrysafi¹ · Alfred Menyhard² · Dimitrios N. Bikiaris³ · Konstantinos Chrissafis¹

Received: 10 January 2020 / Accepted: 16 July 2020 / Published online: 12 August 2020
© Akadémiai Kiadó, Budapest, Hungary 2020

Abstract

Crosslinked high-density polyethylene (PEX) composites containing various amounts of graphite particles (1, 2.5 and 5 mass% or 0.479, 1.206 and 2.445 vol%, respectively) were prepared to study the effect of filler loading on the crystallization behavior of PEX. The crystallization of PEX and its composites was studied using differential scanning calorimetry in non-isothermal crystallization conditions at several cooling rates from 2.5 to 15 K min⁻¹. The crystallization temperature, T_c , of the prepared composites was slightly higher than that of the neat PEX, especially for higher cooling rates, indicating a nucleating effect of graphite filler over the polymer matrix. The experimental data were analyzed using the Avrami modified by Jeziorny method, the Ozawa and the Mo methods. The Avrami modified by Jeziorny and Mo approaches describe more accurately the crystallization of neat PEX and PEX composites while the Ozawa equation fails to describe the non-isothermal crystallization of PEX and its composites. The activation energy (ΔE) of non-isothermal crystallization was calculated using the differential isoconversional method of Friedman. It was found that the introduction of the graphite in the matrix did not modify the crystallization mechanism of PEX. The PEX composite filled with 1 mass% graphite exhibited lower activation energy than neat PEX.

Keywords Crosslinked polyethylene · Graphite particles · Non-isothermal crystallization · Kinetics

Introduction

The interest of the industrial sector is increasingly focused on new types of polyethylene (PE) materials such as crosslinked or branched polyethylene. PE is one of the most widely used polyolefins in many application areas due to its attractive properties such as low cost production, high corrosion resistance, light weight and easy processing techniques

[1]. Physical or chemical crosslinking of polyethylene can lead to improved properties regarding the resistance to thermal degradation, chemical resistance and mechanical properties among others [2]. Crosslinking of polyethylene can be employed using three main crosslinking methods: (1) radiation crosslinking, (2) peroxide crosslinking and (3) silane crosslinking which is cost-effective and industrially applicable, resulting at the same time a high crosslinking degree of polyethylene [3].

Mechanical and thermal properties of crosslinked polyethylene synthesized with various methods have been extensively studied. More specifically, Sen et al. [4] have examined the grafting reaction kinetics, melting behavior and thermal properties of silane-crosslinked LDPE (XLPE). Shieh et al. [5] have studied the silane grafting and crosslinking reactions of LDPE, HDPE and LLDPE, comparing the crosslinking degrees of each polyethylene. Silane-crosslinked HDPE (PEX) has been also studied in terms of its structural and thermal properties by Roumeli et al. [6]. According to Melo et al. and Oliveira et al. [7, 8], crosslinked polyethylene presents enhanced thermal

✉ Dimitra Kourtidou
dikourti@physics.auth.gr

¹ Advanced Materials and Devices Laboratory, School of Physics, Aristotle University of Thessaloniki, 541 24 Thessaloniki, Greece

² Laboratory of Plastics and Rubber Technology, Department of Physical Chemistry and Materials Science, Budapest University of Technology and Economics, Műegyetem Rkp. 3, Budapest 1111, Hungary

³ Laboratory of Organic Chemical Technology, Department of Chemistry, Aristotle University of Thessaloniki, 541 24 Thessaloniki, Greece

stability and mechanical properties compared to the non-crosslinked systems. Thus, PEX has a higher operating limit compared to common HDPE due to its three-dimensional network structure. Currently, PEX is massively produced and employed in many applications such as piping materials, cables and wires, heat shrinkable materials and steam resistant for food packaging [8]. However, the main disadvantage of PEX is the low thermal conductivity which limits its application, especially regarding piping systems used for heating and cooling applications.

To further broaden the application fields of PEX polymer and improve its properties, composite polymer materials have been produced and studied. These multiphase polymer systems present enhanced physicochemical properties depending on the filler material, morphology and its content in the matrix [9–11]. It has been shown that the use of carbon and its allotropic forms, at both micro- and nanosize as a filler in a polymer matrix, can lead to enhanced physical, thermal, mechanical and electrical properties of the matrix [12–18]. Graphite is one of the hardest materials found in nature and has excellent strength and outstanding thermal and electrical conductivity [12] making it an attractive candidate as a filler material for the synthesis of composite polymers with superior properties. PEX composites filled with carbon nanotubes and nanodiamonds have been extensively studied [19–22] regarding their structural, thermal and mechanical properties. It was found that the PEX composites filled with carbon nanotubes and nanodiamonds present higher thermal stability and thermal conductivity and improved mechanical properties compared to neat PEX. Nevertheless, graphite particles are cost-effective compared to the high prices of carbon nanotubes, graphene and nanodiamonds which eventually increase the cost of the industrial scale production of polymer composites. PEX/graphite composites are synthesized and studied for the first time in this work, since no study on such composites has been conducted, to the author's knowledge.

Many studies have been published regarding the isothermal and non-isothermal crystallization of polyethylene composites [23–25] because the crystallization process influences the crystal structure and morphology, and thus the properties of the final material. It has been reported that solid-state particles in a polymer matrix can induce heterogeneous nucleation during the crystallization process resulting in an improved crystallization rate [26–30]. However, according to the literature, crystallization studies on crosslinked polyethylene are mostly focused on crosslinked LDPE and LLDPE [31–34], while crystallization studies of crosslinked polyethylene composites are limited [35]. It is important to notice that no crystallization kinetics study has been conducted for composites with PEX as a matrix, to the knowledge of the authors.

The main scope of this work is to examine the effect of graphite loading on PEX non-isothermal crystallization at various cooling rates from 2.5 to 15 K min⁻¹. Therefore, PEX composites with 1, 2.5 and 5 mass% of graphite micro-particles (0.479, 1.206 and 2.445 vol%, respectively) were prepared by the melt mixing method. The non-isothermal crystallization kinetics of neat PEX and its composites was investigated using the Avrami modified by Jeziorny method and Ozawa equations as well as the method proposed by Mo. Furthermore, the effective crystallization activation energy as a function of the relative degree of crystallinity was calculated using the isoconversional Friedman method.

Experimental

Materials

Chemically crosslinkable high-density polyethylene compound made by silane-grafted ethylene polymer was kindly provided by SILON (Planá nad Lužnicí, Czech Republic) under the trade name of TABOREX TA 1132 HD. It has a melt flow index of 1.9 g × 10 min⁻¹ and 1000 kg × m⁻³ density. A catalyst masterbatch containing the crosslinking catalyst and a stabilizer package was also supplied by SILON under the trade name of TABOREX TA 2111 HD with a melt flow index of 5.5 g × 10 min⁻¹ and 965 kg × m⁻³ density. This catalyst batch can accelerate either the hydrolysis reaction of the grafted silyl groups leading to the formation of silanols or the reaction condensation of silanols to form Si–O–Si bond, or both.

Spherical graphite filler under the trade name GraphTHERM[®] was supplied by Georg H. Luh Company (Walluf, Germany). The average diameter of the particles was 23 μm, and they have a C-content of 99.9%.

Composites preparation

PEX composites were prepared by the melt mixing method. Mixtures of 95 mass% grafted HDPE and 5 mass% of crosslinking catalyst together with 1, 2.5 and 5 mass% (0.479, 1.206 and 2.445 vol%, respectively) graphite filler were physically mixed. Afterward, each of the mixture was melt mixed in a Haake–Buchler Reomixer (model 600) with roller blades and a mixing head with a volumetric capacity of 6.9 × 10⁻⁵ m³ for 600 s at 468 K with a torque speed of 30 rpm. The prepared samples were immediately molded using an Otto Weber, Type PW 30 hydraulic hot press connected with an Omron E5AX Temperature Controller, at a temperature of 453 ± 5 K, in order to prepare films of 350–450 μm thickness. The crosslinking process in the bulk of the polymer was completed by immersing the prepared

films in a hot bath at 363 K for 24 h. The composites samples are referred to this manuscript as PEX/THERM.

Characterization method

Non-isothermal crystallization of the PEX/THERM composites was studied using a differential scanning calorimeter (DSC) Pyris Diamond from PerkinElmer, in a nitrogen atmosphere. To achieve the optimal thermal contact between the sample and the sample container, a rectangular aluminum foil was used to wrap each sample. An aluminum foil of the same dimensions and wrapped the same way was used on the reference holder. The samples were weighed about 4 ± 0.5 mg, and their thermal history was erased by heating from 323 to 473 K at a heating rate of 10 K min^{-1} and staying at this temperature for 5 min. During non-isothermal crystallization measurements, the samples were cooled to 323 K at cooling rates of 2.5, 5, 10 and 15 K min^{-1} .

Results and discussion

Crystallization behavior of PEX and PEX/THERM composites

The effect of graphite loading on the non-isothermal crystallization behavior of PEX was carried out using DSC. The cooling curves of neat PEX and PEX/THERM composites at cooling rates of 2.5, 5, 10 and 15 K min^{-1} are shown in Fig. 1. In all cases, the curves present one exothermal

peak. At the lowest rates ($2.5, 5 \text{ K min}^{-1}$), narrow crystallization peaks appear for all samples, while wider crystallization curves are induced by the highest cooling rates ($10, 15 \text{ K min}^{-1}$). It can be seen that the curves and the crystallization peaks shift to lower temperatures as the cooling rate increases. This is due to the shorter time for the nuclei formation at higher cooling rates. The polymer molecular chains have limited mobility, and thus, the diffusion and chain configuration into more perfect crystallites become more difficult for higher cooling rates [25]. The crystallization peak temperature (T_c) and the crystallization enthalpy (ΔH_c) of neat PEX and PEX/THERM composites are presented in Table 1. Figure 2 shows the crystallization peak temperature of PEX and its composites versus the cooling rate. It is observed that the crystallization peak temperature of PEX composites is slightly higher than that of neat PEX at a given cooling rate, especially for the cooling rates of 10 and 15 K min^{-1} . This indicates that the presence of the graphite particles in the PEX matrix can induce heterogeneous nucleation by creating nucleation sites for the polymer chains, during the crystallization from the melt [36, 37], which is heightened at higher cooling rates.

Non-isothermal crystallization kinetics of neat PEX and PEX/THERM composites

The crystallization heat can be transformed into the relative degree of crystallinity (X_T) by the division of the heat at each crystallization temperature T (ΔH_T) by the total heat (ΔH_0) corresponding to complete crystallization [38]:

Fig. 1 DSC cooling curves at cooling rates from 2.5 to 15 K min^{-1} of **a** neat PEX, **b** PEX/1 THERM, **c** PEX/2.5 THERM, and **d** PEX/5 THERM composites

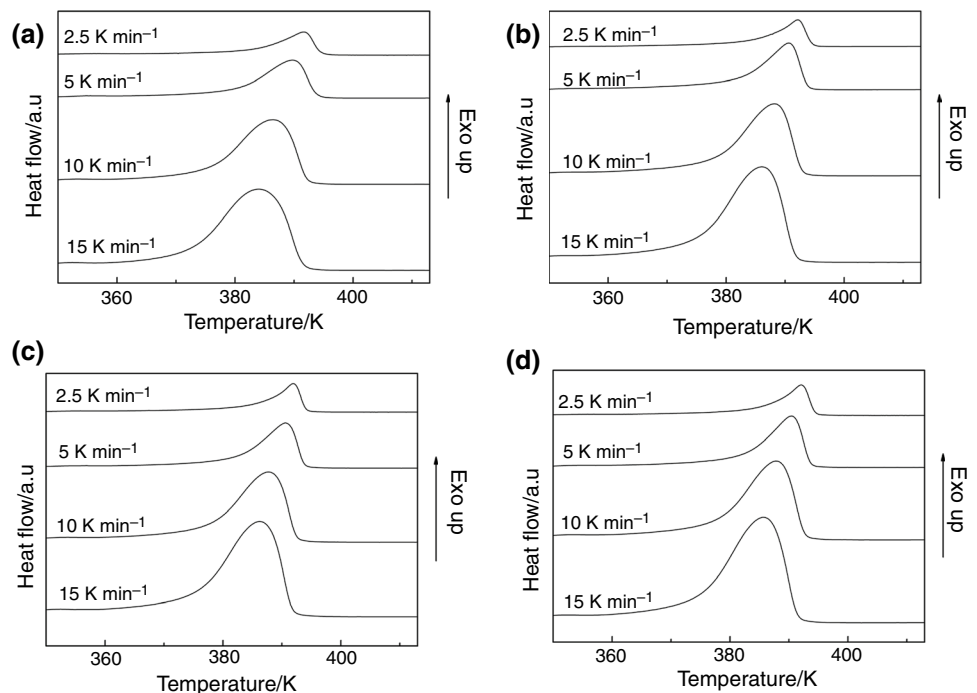


Table 1 Crystallization temperature T_c and the crystallization enthalpy ΔH_c of neat PEX and PEX/THERM composites, under non-isothermal conditions

Cooling rate/ $K\ min^{-1}$	PEX		PEX/1 THERM		PEX/2.5 THERM		PEX/5 THERM	
	T_c/K	$\Delta H_c/J\ g^{-1}$	T_c/K	$\Delta H_c/J\ g^{-1}$	T_c/K	$\Delta H_c/J\ g^{-1}$	T_c/K	$\Delta H_c/J\ g^{-1}$
2.5	391.6	-158.1	392.2	-154.2	391.9	-156	392.1	-156.6
5	389.8	-156.1	390.6	-153.3	390.6	-161.3	390.4	-154.4
10	386.4	-152.9	388.3	-155.4	387.8	-159.7	387.8	-154.9
15	384.2	-160.1	386	-158.7	386.2	-157.3	385.7	-153.3

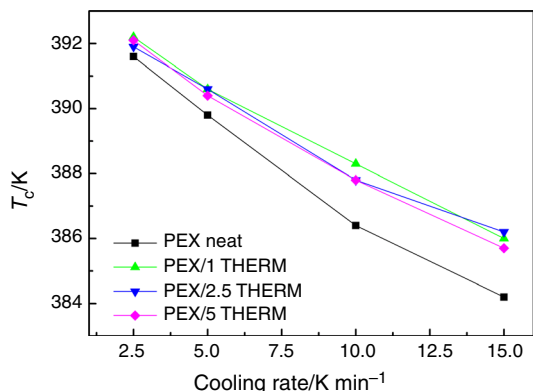


Fig. 2 Crystallization temperature of neat PEX and PEX/THERM composites versus cooling rate

$$X_T = \frac{\int_{T_0}^{T_c} \left(\frac{dH}{dT}\right) dT}{\int_{T_0}^{T_\infty} \left(\frac{dH}{dT}\right) dT} \tag{1}$$

where T_0 , T_c and T_∞ are the initial and final crystallization temperature at time t and the ultimate crystallization temperature, respectively, and dH is the crystallization enthalpy released during an infinitesimal temperature interval dT . The crystallization time t can be derived by the crystallization temperature using the following equation:

$$t = \frac{T_0 - T}{\Phi} \tag{2}$$

where T_0 and T are the temperature at the beginning and at crystallization time t , respectively, and Φ is the cooling rate. The relative degree of crystallinity X_T as a function of time t and temperature T is shown in Fig. 3.

There is a strong dependence of the crystallization process on the cooling rate as it can be seen from these curves. As the crystallization progresses, the curves tend to resemble a flat line because of the spherulite impingement and crowding [39]. The time needed for the crystallization to complete becomes shorter as the cooling rate increases [40–42].

The half time crystallization $t_{1/2}$ as a function of cooling rate Φ of neat PEX and its composites was calculated as shown in Fig. 3, as the time from the onset of crystallization to the time at which the relative degree of

crystallinity reaches 50%, shown in Fig. 4. The $t_{1/2}$ value of PEX/THERM composites is slightly lower compared to neat PEX at a given rate, which is more noticeable at lower cooling rates. This indicates that the addition of the graphite filler accelerates the time needed for the polymer to reach the half degree of crystallization leading to higher crystallization rate by inducing heterogeneous nucleation as shown in Fig. 2. However, it seems that the filler loading does not affect the value of $t_{1/2}$.

The Avrami equation is usually applied to describe the isothermal crystallization kinetics of polymers [43]:

$$1 - X_t = \exp(-Z_t t^n) \tag{3}$$

where X_t is the relative degree of crystallinity at time t , Z_t is the rate constant for crystallization, and n is the Avrami exponent which provides information on the crystallization mechanism and the shape of the formed crystalline units [43]. The double logarithmic form of Eq. 3 gives the following equation:

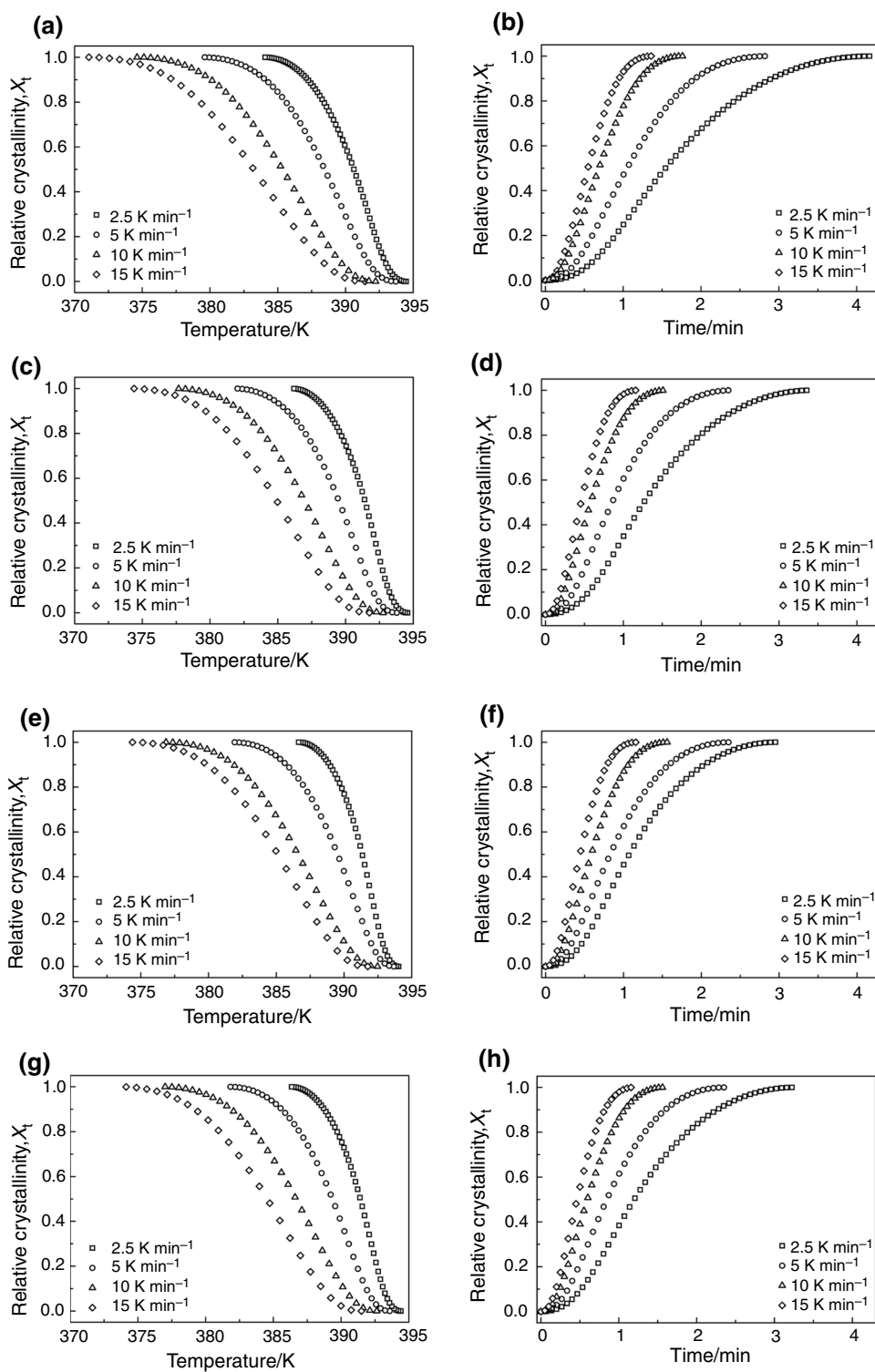
$$\log[-\ln(1 - X_t)] = \log Z_t + n \cdot \log t \tag{4}$$

the plot of $\log[-\ln(1 - X_t)]$ versus $\log t$ for each cooling rate can be obtained. The Avrami exponent n and the rate constant of crystallization Z_t can be determined by the slope and the intercept of the plot, respectively. However, the Avrami approach cannot describe properly the non-isothermal crystallization kinetics. Thus, Jeziorny, considering the non-isothermal character of the process, made an assumption of a constant cooling rate during the crystallization and suggested [44] that the parameter Z_t should be divided by the cooling rate Φ as follows:

$$\log Z_c = \frac{\log Z_t}{\Phi} \tag{5}$$

Figure 5 presents the plots of $\log[-\ln(1 - X_t)]$ versus $\log t$ for neat PEX and PEX/THERM composites at 2.5, 5, 10 and 15 $K\ min^{-1}$. The crystallization area selected in this work was $5\% < X_t < 95\%$. According to Fig. 5, there are two regions of slightly different slopes for all samples, especially at lower cooling rates (2.5, 5 $K\ min^{-1}$). The deviation from linearity is related to a secondary crystallization caused by the impingement of the spherulites on

Fig. 3 Plots of relative crystallinity as a function of temperature: **a** neat PEX, **c** PEX/1 THERM, **e** PEX/2.5 THERM and **g** PEX/5 THERM, and as a function of time: **b** neat PEX, **d** PEX/1 THERM, **f** PEX/2.5 THERM and **h** PEX/5 THERM for non-isothermal crystallization at cooling rates from 2.5 to 15 K min⁻¹



later stages of the crystallization [45]. The linear fitting of two regions at 2.5 and 5 K min⁻¹ and linear fitting of a single region at 10 and 15 K min⁻¹ were conducted, and the results are shown in Table 2. The Avrami exponent of the first region n_1 is between 2.1 and 2.4 for neat PEX and its composites while n_2 at 2.5 and 5 K min⁻¹ in the

second region, is ranging between 1.9 and 2.3 suggesting a two-dimensional crystal growth [46]. The value of n_1 slightly decreases with increasing cooling rate for all samples, indicating that the nucleation mechanism was less complicated at higher cooling rates due to the shorter crystallization time [47]. Since the value of the Avrami

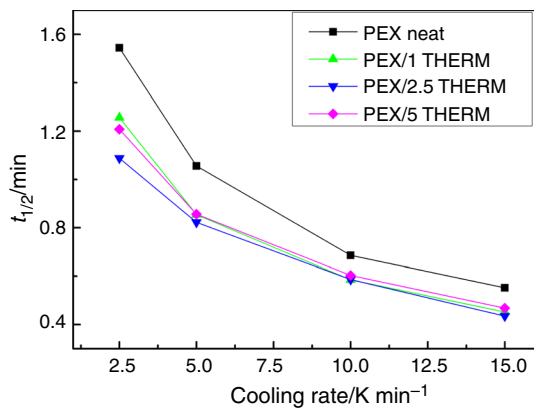


Fig. 4 Half time crystallization $t_{1/2}$ of neat PEX and its composites versus cooling rate

exponent of PEX/THERM composites does not deviate significantly compared to those of neat PEX, it is concluded that the presence of the graphite particles does not affect the nucleation mechanism of the PEX matrix. Furthermore, the values of both Z_{c1} and Z_{c2} parameters of the

studied materials increase with increasing cooling rate for neat PEX and its composites due to the higher crystallization rate. At low cooling rates (2.5, 5), the Z_c parameter of the PEX/THERM composites is slightly higher compared to that of neat PEX indicating that PEX composites have a higher crystallization rate. The standard errors of the n and Z_c values are lower than 0.01 and 0.005, respectively, and for this reason the uncertainties of these parameters are considered insignificant.

Non-isothermal crystallization kinetics was also analyzed using the Ozawa method. According to the Ozawa theory [48], the non-isothermal crystallization process is a result of infinitely small changes in isothermal crystallization steps and the degree of relative crystallinity at a temperature T can be calculated as follows:

$$1 - X_t = \exp \left[\frac{-K(T)}{\phi^m} \right] \tag{6}$$

where ϕ is the cooling rate, m is the Ozawa exponent that is related to the dimensions of the crystal growth, and $K(T)$ is the crystallization rate constant. Equation (6) can be expressed in a double logarithmic form as:

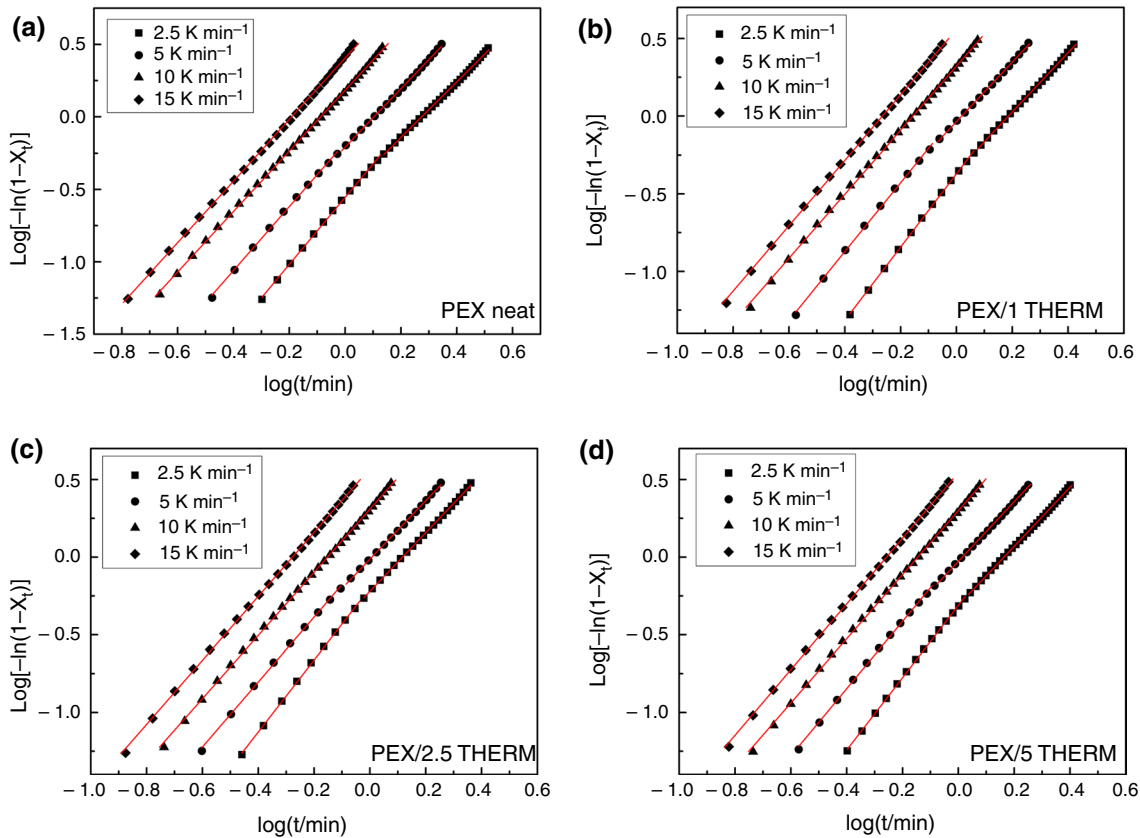


Fig. 5 Plots of $\log [-\ln (1-X_t)]$ versus $\log t$ for the non-isothermal crystallization of **a** neat PEX, **b** PEX/1 THERM, **c** PEX/2.5 THERM, and **d** PEX/5 THERM composites

Table 2 Avrami exponent and Z_c of neat PEX and PEX/THERM composites, under non-isothermal conditions for the linear fitting of two regions at 2.5 and 5 $K\ min^{-1}$ and of a single region at 10 and 15 $K\ min^{-1}$

	Cooling rate/ $K\ min^{-1}$	n_1	Z_{c1}	R_1^2	n_2	Z_{c2}	R_2^2
PEX	2.5	2.3	0.6	0.9991	1.9	0.6	0.999
	5	2.2	0.9	0.999	2	0.9	0.9992
	10	2.1	1	0.9996	–	–	–
	15	2.1	1.1	0.9994	–	–	–
PEX/1 THERM	2.5	2.4	0.7	0.9996	1.9	0.7	0.9991
	5	2.2	1	0.999	1.9	1	0.9992
	10	2.1	1.1	0.9995	–	–	–
	15	2.1	1.1	0.9996	–	–	–
PEX/2.5 THERM	2.5	2.3	0.8	0.9996	1.9	0.8	0.9995
	5	2.1	1	0.9991	1.9	1	0.9992
	10	2	1.1	0.9996	–	–	–
	15	2.1	1.1	0.9996	–	–	–
PEX/5 THERM	2.5	2.3	0.8	0.9995	1.9	0.8	0.9994
	5	2.2	1	0.9991	1.9	1	0.9992
	10	2.1	1.1	0.9995	–	–	–
	15	2.1	1.1	0.9996	–	–	–

$$\log [-\ln (1 - X_t)] = \log K(T) + m \cdot \log \Phi \tag{7}$$

A temperature range is taken into account for each peak of crystallization, in order to obtain the traces from Ozawa’s method. Thus, by drawing the plot of Eq. (7) at a given temperature within this range, a series of straight lines could be obtained, if the Ozawa analysis is adequate to describe the crystallization process. The kinetic parameters m and $K(T)$ can be derived from the slope and the intercept of the plot $\log[-\ln(1 - X_t)]$ versus $\log\Phi$ at a given temperature. The m parameter of neat PEX and PEX/THERM composites increases with increasing temperature. The rate constant $K(T)$ was found to decrease as a result of the slower crystallization of the polymer at higher temperatures (Table 3). However, as shown in Fig. 6, deviation from linearity is observed for all the samples when cooling rates varies, as the coefficient of determination values (R-squared) is lower than 0.98 in most cases. This is due to the fact that, at a given temperature, the crystallization process at different cooling rates is at different stages, i.e., at the lower cooling rate the crystallization process is at its end, while at the higher cooling rate, the crystallization process is in its initial phase. This implies that the Ozawa equation fails to describe the non-isothermal crystallization of PEX and its composites. Also, it is important to note that the Ozawa method ignores secondary crystallization and transcrySTALLIZATION effect [49, 50].

To describe the non-isothermal crystallization process, Mo proposed a combination of the Avrami and Ozawa equations [51]:

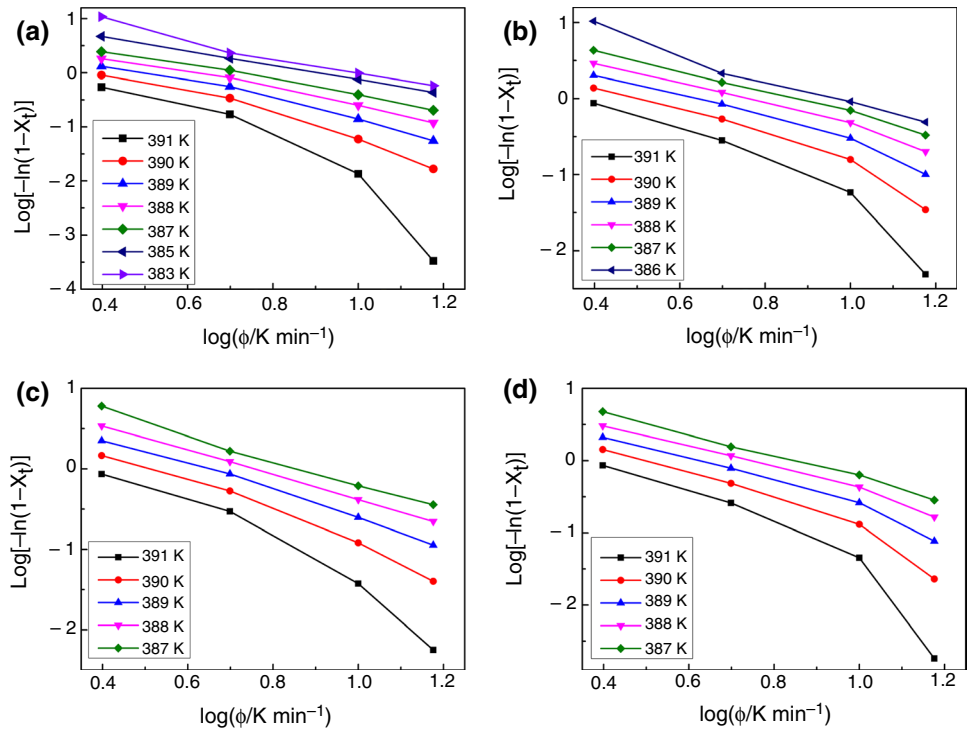
Table 3 Crystallization kinetic parameters based on the Ozawa method for neat PEX and PEX/THERM composites under non-isothermal conditions

	T/K	m	$\log K$	R^2
PEX	389	1.8	0.9	0.984
	388	1.5	0.9	0.99
	387	1.4	1	0.9941
	385	1.3	1.2	0.9998
	383	1.6	1.6	0.9777
PEX/1 THERM	390	2	1	0.954
	389	1.6	1	0.9738
	388	1.5	1.1	0.9872
	387	1.4	1.2	0.9951
	386	1.7	1.6	0.9797
PEX/2.5 THERM	391	2.5	1.2	0.9551
	390	2	1.1	0.9847
	389	1.7	1.2	0.944
	388	1.6	1.3	0.9998
	387	1.8	1.6	0.9943
PEX/5 THERM	391	3.2	1.4	0.8908
	390	2.2	1.1	0.9512
	389	1.8	1.1	0.9743
	388	1.6	1.1	0.9869
	387	1.5	1.3	0.9954

$$\log k + n \cdot \log t = \log K(T) - m \cdot \log \Phi \tag{8}$$

$$\log \Phi = \log F(T) - \alpha \cdot \log t \tag{9}$$

Fig. 6 Plots of $\log[-\ln(1-X_t)]$ versus $\log\Phi$ for the non-isothermal crystallization of **a** neat PEX, **b** PEX/1 THERM, **c** PEX/2.5 THERM, and **d** PEX/5 THERM composites



where $F(T) = [K(T)/Z_t]^{1/m}$, Φ is the cooling rate and α is the ratio between the Avrami and Ozawa exponents n/m . Parameter $F(T)$ has a definite physical and practical meaning and represents the necessary value of cooling rate to reach a certain degree of crystallinity at unit crystallization time [51].

The plots of $\log\Phi$ as a function of $\log t$ at various degrees of crystallinity for neat PEX and PEX/THERM composites are shown in Fig. 7. In all cases, good linearity of the plots is observed since the coefficient of determination values (R-squared) is larger than 0.98 at any case [52, 53]. The

Fig. 7 Plots of the $\log\Phi$ versus $\log t$ for the non-isothermal crystallization of **a** neat PEX, **b** PEX/1 THERM, **c** PEX/2.5 THERM, and **d** PEX/5 THERM composites at specific values of relative crystallinity

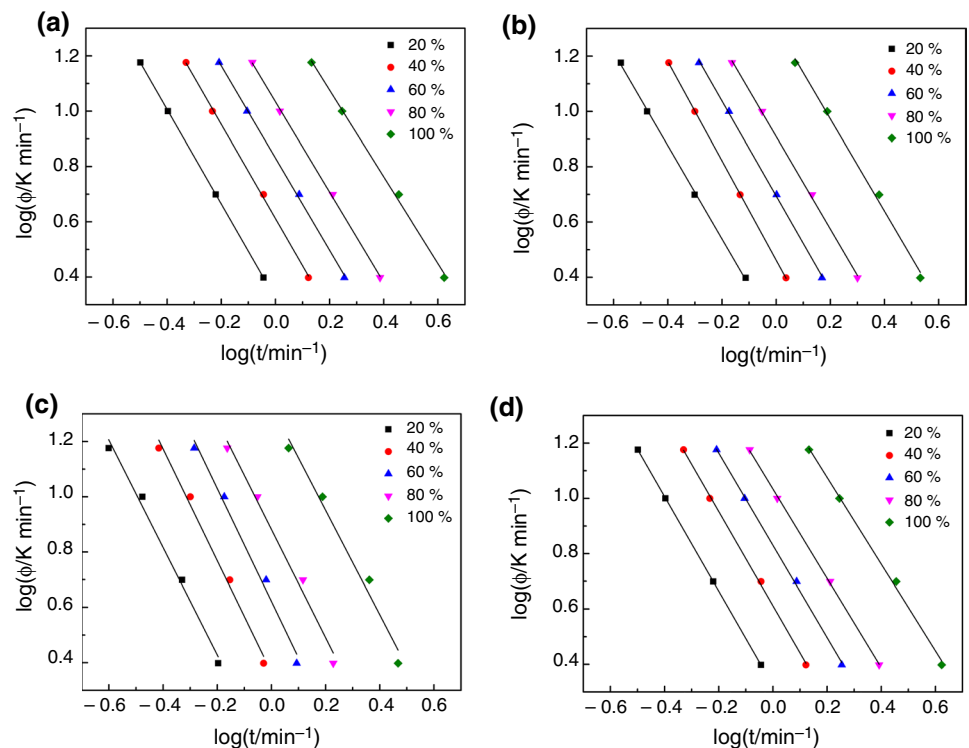


Table 4 Crystallization kinetic parameters based on the Mo method for neat PEX and PEX/THERM composites, under non-isothermal conditions

Relative Crystallinity/%	PEX			PEX/1 THERM			PEX/2.5 THERM			PEX/5 THERM		
	<i>a</i>	log <i>F</i>	<i>R</i> ²	<i>a</i>	log <i>F</i>	<i>R</i> ²	<i>a</i>	log <i>F</i>	<i>R</i> ²	<i>a</i>	log <i>F</i>	<i>R</i> ²
20	1.7	0.3	1	1.7	0.2	0.9993	1.9	0.4	0.9912	1.7	0.3	1
40	1.7	0.6	0.9992	1.8	0.5	1	2	0.4	0.9917	1.7	0.6	0.9992
60	1.7	0.8	0.9991	1.7	0.7	0.9994	1.9	0.6	0.9892	1.7	0.8	0.9991
80	1.6	1	0.9994	1.7	0.9	0.9992	1.9	0.9	0.9876	1.6	1	0.9996
100	1.6	1.4	0.9977	1.7	1.3	0.9961	1.9	1.3	0.9804	1.6	1.4	0.9977

values of parameters α and $F(T)$ were obtained by the intercepts and the slopes of the fitted lines, respectively, as shown in Table 4. It was found that the value of $F(T)$ increases with increasing degree of crystallinity because, at low values of $X(t)$, the polymer matrix is at its melt state and the crystallization rate is high. Furthermore, $F(T)$ parameter of the PEX/THERM composites presents lower values compared to neat PEX until the 60% of relative degree of crystallinity. This indicates that the graphite particles facilitate the crystallization process of PEX composites leading to higher crystallization rates, as it was earlier proposed by the results from the Avrami modified by Jeziorny approach (Table 2). Parameter α remains almost constant for each of the sample at different degrees of crystallinity, and it takes values from 1.6 to 2 similar to the literature results for the crosslinked polyethylene [33].

Crystallization activation energy

Activation energy is the energy required for a phase transformation process to happen. Since there are multiple simultaneous steps during the crystallization process, the activation energy should be described as an effective activation energy [54]. Crystallization of polymers is a process controlled by a dynamic factor associated with the activation energy for the transport of the macromolecular segments to the surface of crystal growth and a static factor related to the free energy barrier for nucleation [55]. The effective activation energy for crystallization is usually evaluated using isoconversional methods. A characteristic isoconversional method to evaluate the dependence of activation energy on the degree of relative crystallinity and temperature during non-isothermal crystallization is Friedman’s method given by the following equation [56]:

$$\ln \left(\frac{dX_t}{dt} \right)_{X_t} = \text{constant} - \frac{\Delta E_{X_t}}{R \cdot T_{X_t}} \tag{10}$$

where dX_t/dt is the instantaneous crystallization rate at a given relative degree of crystallinity X_t , R is the universal gas constant $8314 \text{ J mol}^{-1} \text{ K}^{-1}$, and ΔE_{X_t} is the effective energy

barrier of the crystallization process for a certain value of X_t . By plotting $\ln(dX_t/dt)$ versus $1/T_{X_t}$, the value of $-\Delta E_{X_t}/R$ for a given degree of crystallinity can be obtained by the slope of the fitted line. Figure 8 presents the dependence of the effective activation energy on the degree of relative crystallinity for the neat PEX and PEX/THERM composites. The values of ΔE_{X_t} were found to be negative because the crystallization rate increases as the temperature decreases as a result of the decrease in the free energy barrier to nucleation [25]. Moreover, ΔE_{X_t} increases with increasing relative crystallinity indicating the difficulty of the polymer system to crystallize as the crystallization proceeds. The ΔE_{X_t} values of PEX/1 THERM composite are lower than neat PEX, PEX/2.5 THERM, and PEX/5 THERM composites when the degree of crystallinity is lower than 90% suggesting that the introduction of 1 mass% of the filler accelerates the crystallization process. When X_t value reaches 90%, the ΔE_{X_t} of PEX/1 THERM composite takes almost equal value with the activation energy of neat PEX. The crystallization process is controlled by two stages, nucleation and crystal growth. The graphite particles in the matrix act as nucleation agent making the early stage of crystallization easier. However, when the nuclei have been formed at the later stage of crystallization, the effect of particles on the crystallization process is weakened [38] leading to higher values of ΔE_{X_t} . Composites

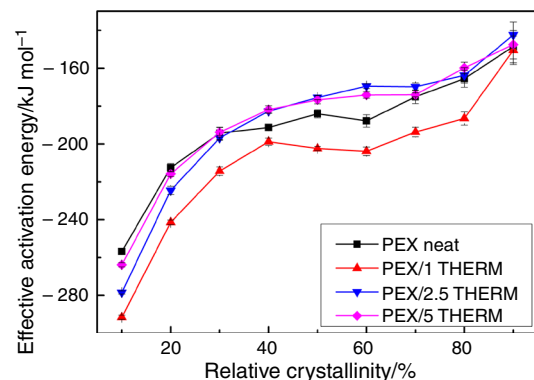


Fig. 8 Dependence of the effective activation energy on the relative crystallinity for PEX and its composites

with 2.5 and 5 mass% filler content present slightly lower ΔE_{X_t} values than neat PEX until 20% degree of relative crystallinity suggesting that the nucleating effect takes place in the early stages of the crystallization, and thus, the presence of the filler facilitates nucleation process. For X_t greater than 20%, the activation energy of PEX/2.5 and PEX/5 THERM composites has almost the same value as neat PEX.

Figure 9 presents the variation in the effective activation energy with the average temperature of neat PEX and PEX/THERM composites at specific X_t for different cooling rates. The value of ΔE_{X_t} increases as the average temperature decreases due to the difficulty of the matrix to crystallize at such low temperatures. It is also observed that the crystallization of PEX/THERM composites begins at slightly higher temperatures compared to neat PEX due to the nucleating effect as was previously suggested.

Using the variation in the ΔE_{X_t} values with the average temperature, the parameters related to crystal growth can be estimated by associating the isoconversional principle with the Hoffman–Lauritzen theory [57]. According to Vyazovkin et al. [58], who combined the Hoffman–Lauritzen theory and the isoconversional approach, the effective activation energy is dependent on the temperature according to the following equation:

$$\Delta E_{X_t} = -R \cdot \frac{d \ln(G)}{dT^{-1}} = U^* \cdot \left(\frac{T^2}{(T - T_\infty)^2} \right) + K_g \cdot R \cdot \left(\frac{(T_m^0)^2 - T^2 - T_m^0 \cdot T}{(T_m^0 - T)^2 \cdot T} \right) \quad (11)$$

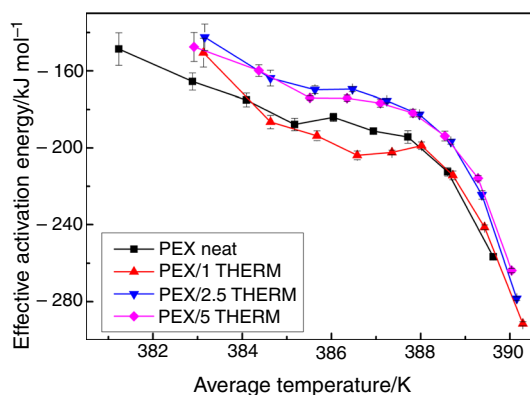


Fig. 9 Dependence of the effective activation energy on the temperature for PEX and its composites

Table 5 Calculated K_g values of PEX and PEX/THERM composites for the two different temperature regions, according to the Hoffman–Lauritzen theory combined with the isoconversional approach

	T range of region A/K	K_g of region A/ K^2	T range of region B/K	K_g of region B/ K^2
PEX	390–386	0.55×10^5	385–381	0.63×10^5
PEX/1 THERM	390–387	0.54×10^5	386–383	0.6×10^5
PEX/2.5 THERM	390–387	0.52×10^5	386–383	0.53×10^5
PEX/5 THERM	390–387	0.51×10^5	386–382	0.55×10^5

where G is the spherulite growth rate, U^* is the activation energy of the segmental jump which characterizes the molecular diffusion across the interfacial boundary between melt and crystalline phases, and is usually set equal to 6.28 kJ mol^{-1} [59]; $T_\infty = T_g - 30$ (where $T_\infty = 135 \text{ K}$ in this work [60, 61]) is the temperature at which the diffusion stops and all segmental motion is frozen, while T_m^0 is taken equal to the equilibrium melting temperature of polyethylene [62] since it has been reported that the crosslinks do not affect the melting point of PE [63]. Using Eq. (11), the Lauritzen–Hoffman parameter K_g can be calculated from the overall rates of non-isothermal crystallization by fitting of the equation above to the experimental data obtained by the isoconversional method of Friedman.

As shown in Fig. 9, the ΔE_{X_t} values of all the samples present a breaking point, and two regions of the effective activation energy dependence on the temperatures are noticeable. For this reason, Eq. (11) was fitted to the experimental data for the two different temperature ranges, for each sample. Table 5 presents the temperature ranges of neat PEX and its composites as well as the calculated values of K_g corresponding to different temperature ranges. It has been reported that a breaking point on the $\Delta E_{X_t}(T)$ dependence could indicate a change in the crystallization

mechanism [64]. However, according to Phillips et al. the crosslinked polyethylene generally follows crystallization regime III [31, 65]. In addition, the ratio of the calculated K_g values derived from the two different regions A and B is almost equal to 1 for all the samples, which is considerably smaller than the theoretical value 2, which corresponds to the change in the crystallization mechanism from regime II to regime III [59]. Therefore, the existence of the breakpoint on the $\Delta E_{X_t}(T)$ plot cannot be assigned to this transition and could be attributed to a change in the crystallographic orientation of the growth front [66].

According to Table 5, the K_g values of PEX/THERM composites present a minor decrease compared to the ones of neat PEX. This indicates that the formation of critical

size of PEX nuclei required slightly less energy in case of the PEX/THERM composites. These results are consistent with the analysis of crystallization kinetics which indicates a higher crystallization rate of PEX composites.

Conclusions

Crosslinked high-density polyethylene composites with various loadings of graphite particles were prepared, in this work, using the melt mixing method. The non-isothermal crystallization kinetics of neat PEX and PEX composites filled with graphite particles was studied using differential scanning calorimetry, for the first time. The incorporation of the graphite particles resulted in a slightly higher crystallization temperatures suggesting a nucleation effect on PEX. Both modified Avrami's and Mo's methods were effective to describe the non-isothermal crystallization of PEX and its composites. Particularly, from the Avrami modified by Jeziorny analysis it is concluded that the incorporation of the graphite particles did not affect the crystallization mechanism of the matrix but resulted in higher crystallization rates of PEX. Mo analysis, which was conducted for the first time for PEX and PEX graphite composites, indicates that the presence of the filler facilitated the crystallization process. The isoconversional method of Friedman was applied in order to evaluate the effective activation energy of the crystallization of PEX and its composites. The incorporation of 1 mass% filler led to lower values of activation energy suggesting that the crystallization of PEX was facilitated. Composites with 2.5 and 5 mass% filler content presented slightly lower ΔE_{Xt} values at low degree of relative crystallinity due to the nucleating effect of the graphite particles. The Hoffman–Lauritzen theory combined with the isoconversional approach was also applied on the experimental data. It was found that the crystallization mechanism was not affected by the incorporation of the filler as was suggested by the Avrami's analysis. K_g parameter of PEX composites presented slightly lower values compared to neat PE suggesting that less energy was needed for the formation of critical size of PEX nuclei in the composites. Further research is currently conducted on the effect of the graphite loading on the thermal conductivity and mechanical properties of PEX and will be presented in a future article.

Acknowledgements This research has been co-financed by the European Union and Greek national funds through the Operational Program Competitiveness, Entrepreneurship and Innovation, under the call RESEARCH–CREATE–INNOVATE (project code: T1EDK- 02611).

Authors contribution All authors contributed to the study conception and design. Material preparation was performed by DK and DNB, data collection was performed by IC and AM, and analysis was performed by DK, ET and KC. This study was supervised by professor Dr. KC.

The first draft of the manuscript was written by DK, and all authors commented on previous versions of the manuscript. All authors read and approved the final manuscript.

Compliance with ethical standard

Conflict of interest The authors declare that they have no conflict of interest.

References

1. Khanam PN, AlMaadeed MAA. Processing and characterization of polyethylene-based composites. *Adv Manuf Polym Compos Sci.* 2015;1:63–79.
2. Patterson R, Kandelbauer A, Müller U, Lammer H. Crosslinked Thermoplastics. *Handb. Thermoset Plast.* 2013.
3. Kurtz S, Manley M. Cross-Linked Polyethylene. *Surg Treat Hip Arthritis Reconstr Replace Revis.* 2009;456–67.
4. Sen AK, Mukherjee B, Bhattacharyya AS, De PP, Bhowmick AK. Kinetics of silane grafting and moisture crosslinking of polyethylene and ethylene propylene rubber. *J Appl Polym Sci.* 1992;44:1153–64.
5. Shieh YT, Liu CM. Silane grafting reactions of LDPE, HDPE, and LLDPE. *J Appl Polym Sci.* 1999;74:3404–11.
6. Roumeli E, Paraskevopoulos KM, Bikiaris D, Chrissafis K. Effect of high energy ball milling on the structure and mechanical properties of cross-linked high density polyethylene. *J Mater Sci.* 2013;48:6753–61.
7. DeMelo RP, De Aguiar VO, De Marques MFV. Silane crosslinked polyethylene from different commercial PE's: influence of comonomer, catalyst type and evaluation of hlpb as crosslinking coagent. *Mater Res.* 2015;18:313–9.
8. Oliveira GL, Costa MF. Optimization of process conditions, characterization and mechanical properties of silane crosslinked high-density polyethylene. *Mater Sci Eng A.* 2010;527:4593–9.
9. Lee MCH. Effects of polymer-filler adhesion on the properties of polychloroprene elastomers filled with surface-treated fillers. *J Appl Polym Sci.* 1987;33:2479–92.
10. Fu SY, Feng XQ, Lauke B, Mai YW. Effects of particle size, particle/matrix interface adhesion and particle loading on mechanical properties of particulate-polymer composites. *Compos Part B Eng.* 2008;39:933–61.
11. Krishnamoorti R, Vaia RA, Giannelis EP. Structure and dynamics of polymer-layered silicate nanocomposites. *Chem Mater.* 1996;8:1728–34.
12. Naz A, Kausar A, Siddiq M. Influence of graphite filler on physicochemical characteristics of polymer/graphite composites: a review. *Polym Plast Technol Eng.* 2016;55:604–25.
13. Alshammari BA, Al-Mubaddel FS, Karim MR, Hossain M, Al-Mutairi AS, Wilkinson AN. Addition of graphite filler to enhance electrical, morphological, thermal, and mechanical properties in poly (ethylene terephthalate): experimental characterization and material modeling. *Polymers.* 2019;11:1411.
14. Calixto CMF, Mendes RK, de Oliveira AC, Ramos LA, Cervini P, Cavalheiro ÉTG. Development of graphite-polymer composites as electrode materials. *Mater Res.* 2007;10:109–14.
15. Tarani E, Terzopoulou Z, Bikiaris DN, Kyratsi T, Chrissafis K, Vourlias G. Thermal conductivity and degradation behavior of HDPE/graphene nanocomposites: pyrolysis, kinetics and mechanism. *J Therm Anal Calorim.* 2017;129:1715–26.
16. Nagy B, Domán A, Menyhárd A, László K. Influence of graphene oxide incorporation on Resorcinol-formaldehyde polymer and carbon aerogels. *Period Polytech Chem Eng.* 2018;62:441–9.

17. Nagy B, Bakos I, Bertóti I, Domán A, Menyhárd A, Mohai M, et al. Synergism of nitrogen and reduced graphene in the electrocatalytic behavior of resorcinol—formaldehyde based carbon aerogels. *Carbon N Y*. 2018;139:872–9.
18. Mokhena TC, Mochane MJ, Sefadi JS, Motloung SV, Andala DM. Thermal Conductivity of Graphite-Based Polymer Composites. *Impact Therm Conduct Energy Technol*. 2018.
19. Roumeli E, Pavlidou E, Bikiaris D, Chrissafis K. Microscopic observation and micromechanical modeling to predict the enhanced mechanical properties of multi-walled carbon nanotubes reinforced crosslinked high density polyethylene. *Carbon N Y*. 2014;67:475–87.
20. Roumeli E, Pavlidou E, Avgeropoulos A, Vourlias G, Bikiaris DN, Chrissafis K. Factors controlling the enhanced mechanical and thermal properties of nanodiamond-reinforced cross-linked high density polyethylene. *J Phys Chem B*. 2014;118:11341–52.
21. Roumeli E, Markoulis A, Kyratsi T, Bikiaris D, Chrissafis K. Carbon nanotube-reinforced crosslinked polyethylene pipes for geothermal applications: from synthesis to decomposition using analytical pyrolysis-GC/MS and thermogravimetric analysis. *Polym Degrad Stab*. 2014;100:42–53.
22. Roumeli E, Avgeropoulos A, Pavlidou E, Vourlias G, Kyratsi T, Bikiaris D, et al. Understanding the mechanical and thermal property reinforcement of crosslinked polyethylene by nanodiamonds and carbon nanotubes. *RSC Adv*. 2014;4:45522–34.
23. Zou P, Tang S, Fu Z, Xiong H. Isothermal and non-isothermal crystallization kinetics of modified rape straw flour/high-density polyethylene composites. *Int J Therm Sci*. 2009;48:837–46.
24. Wu Z, Zhang Z, Mai K. Non-isothermal crystallization kinetics of UHMWPE composites filled by oligomer-modified CaCO₃. *J Therm Anal Calorim*. 2019;0123456789.
25. Tarani E, Wurm A, Schick C, Bikiaris DN, Chrissafis K, Vourlias G. Effect of graphene nanoplatelets diameter on non-isothermal crystallization kinetics and melting behavior of high density polyethylene nanocomposites. *Thermochim Acta*. 2016;643:94–103.
26. Qiu Z, Li Z. Effect of orotic acid on the crystallization kinetics and morphology of biodegradable poly(l-lactide) as an efficient nucleating agent. *Ind Eng Chem Res*. 2011;50:12299–303.
27. Chen K, Yu J, Qiu Z. Effect of low octavinyl-polyhedral oligomeric silsesquioxanes loading on the crystallization kinetics and morphology of biodegradable poly(ethylene succinate-co-5.1 mol% ethylene adipate) as an efficient nucleating agent. *Ind Eng Chem Res*. 2013;52:1769–74.
28. Yu J, Qiu Z. Preparation and properties of biodegradable poly(L-lactide)/octamethyl-polyhedral oligomeric silsesquioxanes nanocomposites with enhanced crystallization rate via simple melt compounding. *ACS Appl Mater Interfaces*. 2011;3:890–7.
29. Sun H, Yang X, Wei K, Wu Y, Fang W. Non-isothermal crystallization kinetics of continuous glass fiber-reinforced poly(ether ether ketone) composites. *J Therm Anal Calorim*. 2019;138:369–78.
30. Mata-Padilla JM, Ávila-Orta CA, Almendárez-Camarillo A, Martínez-Colunga JG, Hernández-Hernández E, Cruz-Delgado VJ, et al. Non-isothermal crystallization behavior of isotactic polypropylene/copper nanocomposites. *J Therm Anal Calorim*. 2020.
31. Phillips PJ, Kao YH. Crystallinity in chemically crosslinked low density polyethylenes: 2. Crystallization kinetics. *Polymer*. 1986;27:1679–86.
32. Jiao C, Wang Z, Liang X, Hu Y. Non-isothermal crystallization kinetics of silane crosslinked polyethylene. *Polym Test*. 2005;24:71–80.
33. Wu H, Liang M, Lu C. Non-isothermal crystallization kinetics of peroxide-crosslinked polyethylene: effect of solid state mechanochemical milling. *Thermochim Acta*. 2012;545:148–56.
34. Phillips PJ, Lambert WS. Regime transitions in a nonreptating polymer: cross-linked linear polyethylene. *Macromolecules*. 1990;23:2075–81.
35. Jose JP, Chazeau L, Cavallé JY, Varughese KT, Thomas S. Nucleation and nonisothermal crystallization kinetics in cross-linked polyethylene/zinc oxide nanocomposites. *RSC Adv*. 2014;4:31643–51.
36. Pustak A, Pucić I, Denac M, Švab I, Pohleven J, Musil V, et al. Morphology of polypropylene/silica nano- and microcomposites. *J Appl Polym Sci*. 2013;128:3099–106.
37. Pagé DJYS, Gopakumar TG. Properties and crystallization of maleated polypropylene/graphite flake nanocomposites. *Polym J*. 2006;38:920–9.
38. Wang S, Zhang J. Non-isothermal crystallization kinetics of high density polyethylene/titanium dioxide composites via melt blending. *J Therm Anal Calorim*. 2014;115:63–71.
39. Peng Z, Kong LX, Li SD. Non-isothermal crystallisation kinetics of self-assembled polyvinylalcohol/silica nano-composite. *Polymer*. 2005;46:1949–55.
40. Jain S, Goossens H, Van Duin M, Lemstra P. Effect of in situ prepared silica nano-particles on non-isothermal crystallization of polypropylene. *Polymer*. 2005;46:8805–18.
41. Kim JY, Park HS, Kim SH. Unique nucleation of multi-walled carbon nanotube and poly(ethylene 2,6-naphthalate) nanocomposites during non-isothermal crystallization. *Polymer*. 2006;47:1379–89.
42. Zheng L, Wang YZ, Yang KK, Wang XL, Chen SC, Li J. Effect of PEG on the crystallization of PPDO/PEG blends. *Eur Polym J*. 2005;41:1243–50.
43. Di Lorenzo ML, Silvestre C. Non-isothermal crystallization of polymers. *Sci: Prog. Polym*; 1999.
44. Jeziorny A. Parameters characterizing kinetics of nonisothermal crystallization of poly(ethylene-terephthalate) determined by DSC. *Polymer*. 1978;19:1142–4.
45. Cebe P, Hong SD. Crystallization behaviour of poly(ether-etherketone). *Polymer*. 1986;27:1183–92.
46. Ho Lam RS, Rogers MA. Experimental validation of the modified Avrami model for non-isothermal crystallization conditions. *CrystEngComm*. 2011;13:866–75.
47. Kuo MC, Huang JC, Chen M. Non-isothermal crystallization kinetic behavior of alumina nanoparticle filled poly(ether ether ketone). *Mater Chem Phys*. 2006;99:258–68.
48. Ozawa T. Kinetics of non-isothermal crystallization. *Polymer*. 1971;12(3):150.
49. Eder M, Wlochowicz A. Kinetics of non-isothermal crystallization of polyethylene and polypropylene. *Polymer*. 1983;24:1593–5.
50. Weng W, Chen G, Wu D. Crystallization kinetics and melting behaviors of nylon 6/foiled graphite nanocomposites. *Polymer*. 2003;44:8119–32.
51. Liu T, Mo Z, Wang S, Zhang H. Isothermal melt and cold crystallization kinetics of poly(aryl ether ether ketone) (PEEKK). *Eur Polym J*. 1997;33:1405–14.
52. Layachi A, Makhlof A, Frihi D, Satha H, Belaadi A, Seguela R. Non-isothermal crystallization kinetics and nucleation behavior of isotactic polypropylene composites with micro-talc. *J Therm Anal Calorim*. 2019;138:1081–95.
53. Fang J, Lang M, Ye X, Zhang W, Zhu K. Non-isothermal crystallization behavior of polypropylene/zinc oxide composites. *Sci Eng Compos Mater*. 2016;23:505–10.
54. Bin-Dahman OA, Shehzad F, Al-Harhi MA. Influence of graphene on the non-isothermal crystallization kinetics of poly(vinyl alcohol)/starch composite. *J Polym Res*. 2018;25.
55. Yuan Q, Awate S, Misra RDK. Nonisothermal crystallization behavior of polypropylene-clay nanocomposites. *Eur Polym J*. 2006;42:1994–2003.

56. Friedman HL. Kinetics of thermal degradation of char-forming plastics from thermogravimetry. Application to a phenolic plastic. *J Polym Sci Part C Polym Symp.* 2007;6:183–95.
57. Lauritzen JI, Hoffman JD. Extension of theory of growth of chain-folded polymer crystals to large undercoolings. *J Appl Phys.* 1973;44:4340–52.
58. Vyazovkin S, Sbirrazzuoli N. Isoconversional approach to evaluating the Hoffman-Lauritzen parameters (U^* and K_g) from the overall rates of nonisothermal crystallization. *Macromol Rapid Commun.* 2004;25:733–8.
59. Jacobs K. *Treatise on solid state chemistry. Volume 3: Crystalline and noncrystalline solids.* Krist. und Tech. 1977.
60. Khonakdar HA, Morshedian J, Wagenknecht U, Jafari SH. An investigation of chemical crosslinking effect on properties of high-density polyethylene. *Polymer.* 2003;44:4301–9.
61. Khonakdar HA, Jafari SH, Hässler R. Glass-transition-temperature depression in chemically crosslinked low-density polyethylene and high-density polyethylene and their blends with ethylene vinyl acetate copolymer. *J Appl Polym Sci.* 2007;104:1654–60.
62. Wunderlich B, Czornyj G. A study of equilibrium melting of polyethylene. *Macromolecules.* 1977;10:906–13.
63. Mandelkern L. *Crystallization of Polymers.* Cambridge: Cambridge University Press; 2001.
64. Vyazovkin S, Stone J, Sbirrazzuoli N. Hoffman-Lauritzen parameters for non-isothermal crystallization of poly(ethylene terephthalate) and poly(ethylene oxide) melts. *J Therm Anal Calorim.* 2005;80:177–80.
65. Scott Lambert W, Phillips PJ, Lin JS. Small-angle X-ray scattering studies of crystallization in crosslinked linear polyethylene. *Polymer.* 1994;35:1809–18.
66. Point JJ, Damman P, Janimak JJ. Is the break in the curve giving the thermal dependence of crystal growth rate a signature of regime II \rightarrow III transition? *Polymer.* 1993;34:3771–3.

Publisher's Note Springer Nature remains neutral with regard to jurisdictional claims in published maps and institutional affiliations.